CHAPTER 6 An overview of the effects of radiation and convection

6.1 Convective energy transports

Riehl and Malkus (1958; Fig. 6.1) argued from the observed energy balance and vertical structure of the tropical atmosphere that deep, penetrative cumulus convection is the primary mechanism for upward energy transport in the tropics. They began by estimating the mass circulation across a latitude 10° on the winter side of the intertropical convergence zone (ITCZ). Recall that the "body" of the main solstitial Hadley Cell lies in the winter hemisphere. They neglected the mass transport across the boundary of the ITCZ on the summer side. They then attempted to evaluate the lateral energy transports across into and out of the ITCZ, as functions of height. They considered transports of internal energy, potential energy, and latent energy. Because the low-level inflow is warm and wet, while the upper level outflow is cold and dry, both internal and latent energy flow in to the ITCZ; nevertheless there is a net loss of

Figure 6.1: Joanne Malkus (now Joanne Simpson), and the late Herbert Riehl.

total energy due to the export of potential energy in the elevated outflow layer. The next export of energy by the meridional flow implies that there is a compensating net input of energy at the top and bottom of the column. Their estimates of the various quantities are summarized in Table 6.1.

Because energy flows into the ITCZ at low levels, and out at high levels, Riehl and Malkus concluded that there must be a net upward transport of energy inside the ITCZ. They argued, however, that this upward energy flux cannot be due to the mean flow, because the observed profile of moist static energy has a minimum at mid levels, as discussed in Chapter

2. If the mean flow was acting alone, then since h is conserved following parcels h would be uniform with height throughout the ascending column. Similar reasoning shows that diffusive energy transport cannot explain the observed upward energy flux. Riehl and Malkus concluded that the upward energy transport must occur in deep convective clouds that penetrate through the troposphere.

Table 6.1: Lateral energy transports on the poleward side of the ITCZ. Adapted from Riehl and Malkus (1958).

δp *100s mb*	v *m s^{-1}*	M_0 *10^{13} g s^{-1}*	s *J g^{-1}*	sM_0 *10^{16} J s^{-1}*	Lq *J g^{-1}*	LqM_0 *10^{16} J s^{-1}*	hM_0 *10^{16} J s^{-1}*	*Eddy moisture transport, 10^{16} J s^{-1}*	*Total energy transport out of the ITCZ, 10^{16} J s^{-1}*
10-9	-1.3	-5.2	301.5	-1.56	37.6	-0.20			
9-8	-1.1	-4.4	305.7	-1.34	27.6	-0.12			
8-7	-0.4	-1.6	311.6	-0.49	18.4	-0.03			
7-6	0	0	317.8	0	11.3	0			
6-5	0	0	323.3	0	7.1	0			
5-4	0.3	1.2	329.1	0.39	4.2	0.00			
4-3	0.6	2.4	335.4	0.80	2.1	0.00			
3-2	1.3	5.2	340.8	1.77	0.8	0.00			
2-1.25	0.8	2.4	348.4	0.83	0	0			
10--5				-3.39		-0.35	-3.74	0.07	-3.67
5-1.25				3.79		0.01	3.80	0	3.80
10-1.25				0.40		-0.34	0.06	0.07	0.13

Neelin and Held (1987) considered the moist static energy budget of the ITCZ from a similar perspective. In a time average, the vertically integrated moist static energy budget is expressed by

$$g^{-1}\nabla \bullet \left(\int_0^{p_S} \mathbf{V} h dp \right) = -(N_S - N_T) , \tag{6.1}$$

where N is the net downward flux of energy due to turbulence, convection and radiation, and subscripts T and S denote the top of the atmosphere and the surface, respectively. Similarly, mass continuity gives

$$\nabla \bullet \left(\int_0^{p_S} \mathbf{V} dp \right) = 0 . \tag{6.2}$$

Divide the column into upper and lower portions, and write

$$p_S^{-1} \nabla \bullet \left(\int_0^{p_S} \mathbf{V} h dp \right) = \nabla \bullet (\mathbf{V}h)_u + \nabla \bullet (\mathbf{V}h)_l = -g \left(\frac{N_S - N_T}{p_S} \right) , \tag{6.3}$$

$$p_S^{-1} \nabla \bullet \left(\int_0^{p_S} \mathbf{V} dp \right) = \nabla \bullet \mathbf{V}_u + \nabla \bullet \mathbf{V}_l = 0 . \tag{6.4}$$

For the tropics, horizontal variations of h are weak, so that it is useful to define h_u and h_l by

$$\nabla \bullet (\mathbf{V}h)_u \equiv h_u (\nabla \bullet \mathbf{V}_u) , \tag{6.5}$$

$$\nabla \bullet (\mathbf{V}h)_l \equiv h_l (\nabla \bullet \mathbf{V}_l) . \tag{6.6}$$

Combining (6.3) - (6.6) gives

$$\nabla \bullet \mathbf{V}_l = \frac{g}{p_S} \left(\frac{N_S - N_T}{h_u - h_l} \right) . \tag{6.7}$$

This shows that low-level convergence ($\nabla \bullet \mathbf{V}_l < 0$) must occur where the column is gaining energy ($N_S - N_T < 0$), provided that

$$h_u - h_l > 0 . \tag{6.8}$$

We note that (6.8) must be satisfied if the upper branch carries energy away faster than the lower branch carries energy in. Neelin and Held call $h_u - h_l$ the "*gross moist stability*." According to (6.7), the pattern of the gross moist stability is closely linked to the pattern of low-level convergence, for a given distribution of $N_T - N_S$. As discussed later [see (6.26)], we expect the gross moist stability to be small where cumulus convection is active.

6.2 Radiative-convective equilibrium

The study of Riehl and Malkus showed that in the tropics (and also in the moist convective regions of the summer hemisphere middle latitudes) upward transport of energy is due to small-scale convection rather than vertical advection by the large-scale vertical motion.

Recall that the brightness temperature of the Earth corresponds to a level in the middle troposphere; the brightness temperature of the tropical convective regions corresponds to the actual temperature in the upper troposphere. We can consider that convection transports energy upward, to the middle or upper troposphere, where radiation can take over and carry the energy on out to space.

The simplest model that can represent this process is called a radiative-convective model. The basic idea is very simple. First, assemble physical parameterizations that suffice to determine the time rates of change of the temperature within the atmospheric column and at the Earth's surface. Combine them into a model, and integrate using a time step on the order of an hour or so. Repeat until a steady state is approached to sufficient accuracy. Depending on the initial conditions, convergence can take on the order of 500 simulated days. No significance is ascribed to the time evolution itself; only the steady state is of interest. It is not obvious a priori that a radiative-convective model will actually approach a steady state, but the models discussed below do.

The physical ingredients of a radiative-convective model include parameterizations of radiation, convection, turbulence, and the processes that determine the change of the surface temperature. We write

$$\rho c_p \frac{\partial T}{\partial t} = LC - \frac{\partial F_s}{\partial z} + Q_R \,. \tag{6.9}$$

Horizontal and vertical advection are deliberately omitted in (6.9), because the purpose of a radiative-convective model is to help us to understand what the atmosphere would look like in their absence. In order to use (6.9), we must determine the condensation rate and the convective fluxes. Obviously this will entail consideration of the moisture budget. In addition, the vertical distributions of water vapor and clouds are needed to determine Q_R, which satisfies

$$Q_R = \frac{\partial}{\partial z}(S - R) \,. \tag{6.10}$$

Here S is the net solar radiation (positive down), and R is the net terrestrial radiation (positive up).

We also impose an energy budget for the Earth's surface:

$$C_g \frac{\partial T_S}{\partial t} = N_S(T_S) \,. \tag{6.11}$$

Here C_g is the effective "heat capacity" of the surface, T_S is the surface temperature, and $N_S(T_S)$ denotes the net downward vertical flux of energy due to turbulence, convection, and radiation. Eq. (6.11) can be used to determine T_S, provided that the functional form of $N_S(T_S)$ is specified. The value of C_g determines how rapidly the surface temperature

changes in response to a given value of N_S. When C_g is large T_S changes slowly. When $C_g \to 0$, T_S adjusts instantaneously so as to keep $N_S(T_s) = 0$.

The radiative-convective balance requirements that must be satisfied in equilibrium can be stated as follows:

- There can be no net radiative energy flux at the top of the atmosphere:

$$N_T = S_T - R_T = 0 . \tag{6.12}$$

- This was discussed in Chapter 1. The atmospheric column must be in energy balance:

$$N_S = N_T , \tag{6.13}$$

where

$$N_S \equiv S_S - R_S - (F_h)_S . \tag{6.14}$$

- From (6.12) - (6.13), it follows that in equilibrium the Earth's surface must also be in energy balance:

$$N_S = 0 . \tag{6.15}$$

We now discuss some results from radiative-convective models. In a series of studies during the 1960s (see bibliography), Manabe and his colleagues investigated the degree to which pure radiative equilibrium and/or radiative-convective equilibrium can explain the observed vertical distribution of temperature. These studies made major advances in our understanding of the vertical structure of the atmosphere. Because little was known about moist physics during the 1960s[1], Manabe et al. did not explicitly represent moist processes in their model; instead, they made alternative assumptions for the vertical distribution of moisture (discussed below), and adopted fairly drastic but empirically justified simplifying assumptions to determine the effects of latent heat release and moist convection on the atmospheric temperature profile.

They used a time-marching method to find equilibrium solutions. Suppose that initial conditions are specified for the temperatures of the atmosphere and surface. From this information, together with a specification of the composition of the atmosphere, it is possible to determine the net radiative cooling of the atmosphere at each level, due to both terrestrial and solar radiation. By integration, we can then determine the net atmospheric radiative cooling, ARC, which is given by

$$ARC = (R_T - R_S) - (S_T - S_S) . \tag{6.16}$$

[1] And only a little more is known now...

Manabe et al. *assumed* that on each time step the net radiative cooling of the atmosphere is equal to the net radiative warming of the surface, i.e.

$$ARC = S_S - R_S . \tag{6.17}$$

From (6.12) and (6.16) it is clear that (6.17) must hold in equilibrium, but it is not logically required during the approach to equilibrium.

Manabe et al. also assumed that on each time step the excess of net downward surface solar radiation over net upward surface longwave radiation equals the net integrated radiative cooling of the atmospheric column. Again, this must really be true only in equilibrium. From (6.14), (6.15), and (6.17), it follows that

$$(F_h)_S = ARC . \tag{6.18}$$

An updated surface temperature can then be determined by time-stepping (6.11) with (6.14).

Manabe et al. imposed (6.15) even during the approach to equilibrium. The physical interpretation of this assumption is that the heat capacity of Earth's surface is zero; in that case, (6.15) follows immediately from (6.11). Realistically, of course, the Earth's surface does have a finite heat capacity (primarily in the ocean), and so (6.15) does not apply at any given instant. Because Manabe et al. were mainly interested in the equilibrium solution anyway, however, their assumption is fairly harmless.

The vertical distribution of ozone is important for the radiation calculation, because it is the absorption of solar radiation by ozone that accounts for the upward increase of temperature in the stratosphere; without ozone, there would be no stratosphere. Manabe and Wetherald did not attempt to compute the vertical distribution of ozone; instead they prescribed it according to observations.

They also had to determine the distribution of water vapor. Although they did not attempt to compute it from a moisture budget (a very serious omission), they did consider two alternative assumptions. The first is fixed specific humidity, and the second is fixed relative humidity. These were both prescribed from observations similar to those shown in Chapter 2. Although Manabe and Wetherald's model does not include a water budget, more modern radiative-convective models do include explicit water budgets. In these models, water vapor is introduced by evaporation from the sea surface; convection and to a much smaller degree diffusion carry the moisture upward; and precipitation removes it. An example will be given later.

A radiative-convective equilibria can be found through the procedure summarized in Fig. 6.2. Initial conditions are given for the vertical profile of atmospheric temperature. After the temperature profile has been modified by radiation, on each time step, the resulting temperature profile is checked for convective stability. Manabe and Wetherald assumed that moist convective instability exists if the temperature decreases upward more rapidly than 6.5 K km^{-1}. If instability is found, the temperature profile is adjusted so as to restore a lapse rate of 6.5 K km^{-1}. The vertical distribution of water vapor is then corrected, using the assumption of either fixed absolute humidity or fixed relative humidity.

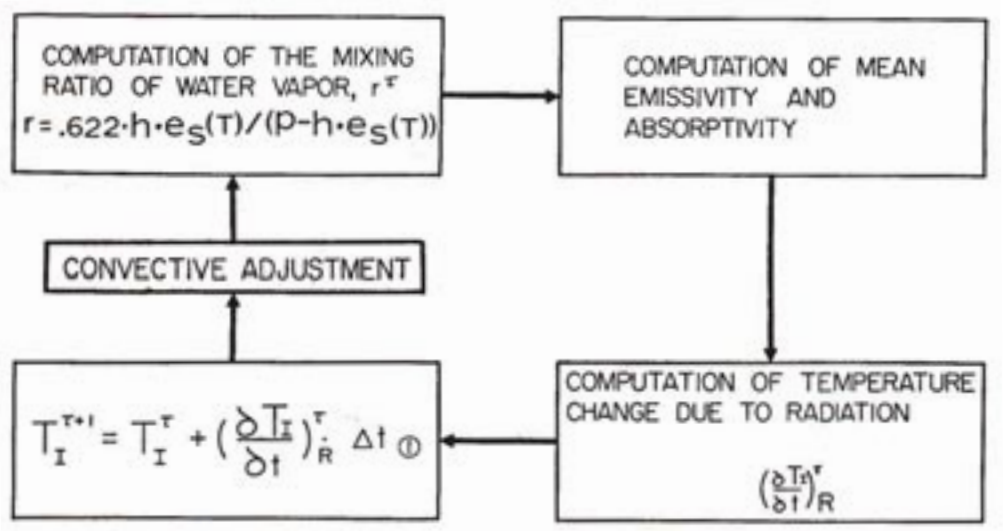

Figure 6.2: Flow chart for the numerical time integration in the radiative - convective equilibrium study of Manabe and Wetherald (1967).

The assumption that the lapse rate "adjusts" to 6.5 K km^{-1} is based on the physical hypothesis that convection acts to prevent the lapse rate from becoming much steeper than the moist adiabatic lapse rate, which is close to 6.5 K km^{-1} in the tropical lower troposphere. The physical meaning of this hypothesis will be discussed further later in this chapter.

Fig. 6.3 shows Manabe and Wetherald's results for three cases:

- pure radiative equilibrium of the clear atmosphere with a given distribution of relative humidity,
- radiative equilibrium of the clear atmosphere with a given distribution of absolute humidity, and
- radiative-convective equilibrium of the atmosphere with a given distribution of relative humidity.

Pure radiative equilibria exhibit a troposphere and a stratosphere, with the tropopause at a fairly realistic height. An unrealistic aspect of both of the radiative equilibria is that the lower troposphere is convectively unstable, even for dry convection. In the radiative-convective calculations, this instability is assumed to be removed by convection. The radiative-convective equilibrium with fixed relative humidity is amazingly realistic, considering that the model ignores all large-scale dynamical processes.

We now present the results of more modern radiative-convective equilibrium calculations performed using the physical parameterizations of the Colorado State University general circulation model. In these simulations, the surface temperature was prescribed according to the observed zonal annual means, and annually averaged insolation was used at each latitude. The model incorporates an elaborate theory of the interactions of cumulus convection with the large-scale circulation (see the next subsection), based on the work of

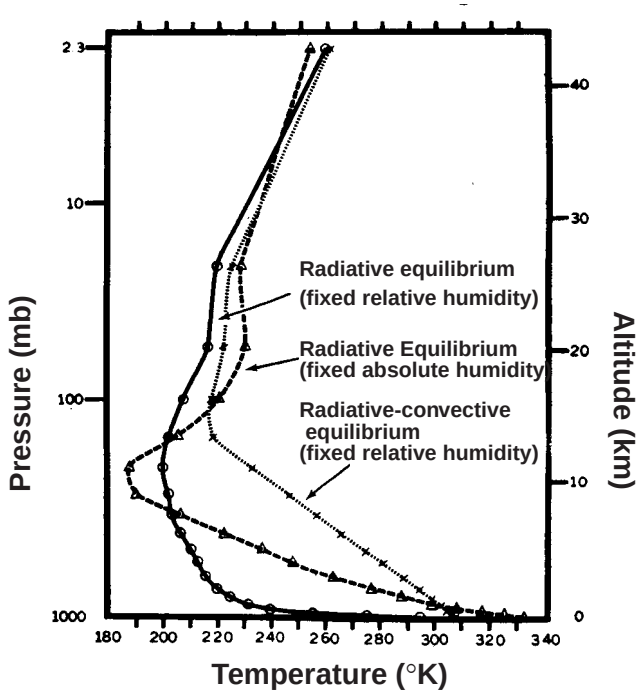

Figure 6.3: **Solid line, radiative equilibrium of the clear atmosphere with a given distribution of relative humidity; dashed line, radiative equilibrium of the clear atmosphere with a given distribution of absolute humidity; dotted line, radiative convective equilibrium of the atmosphere with a given distribution of relative humidity. From Manabe and Wetherald (1967).**

Arakawa and Schubert (1974, discussed in the next sub-section), Randall and Pan (1993), and Pan and Randall (1998) as well as representations of stratiform cloud processes (Fowler et al., 1996) and boundary-layer turbulence (Suarez et al. 1983). A surface wind speed is needed to determine the surface fluxes of sensible and latent heat using bulk aerodynamic formulae similar to those discussed earlier; a value of 5 m s^{-1} was assumed for this purpose. The boundary layer, cumulus, and stratiform cloud parameterizations together determine the equilibrium distribution of moisture. The boundary layer, cumulus, stratiform cloud, and radiation parameterizations determine the distribution of temperature. Clouds in the radiative sense were neglected. The top of the model was placed at 1 mb, and 29 levels were used. Stratospheric ozone amounts were prescribed from observations. Note that in this model the distribution of moisture is predicted; this is a key difference from the work of Manabe and colleagues, discussed above.

Fig. 6.4 shows the results with and without prescribed statospheric ozone. When ozone is present, the model produces a very obvious stratosphere in which the temperature increases upward; when ozone is neglected, on the other hand, the upper regions of the model atmosphere become more or less isothermal. The structure of the tropospheric temperature sounding is only slightly altered by the effects of stratospheric ozone.

Fels (1985) reported the results of similar radiative-convective equilibria on the sphere, but his model included a representation of photochemistry, and he emphasized the

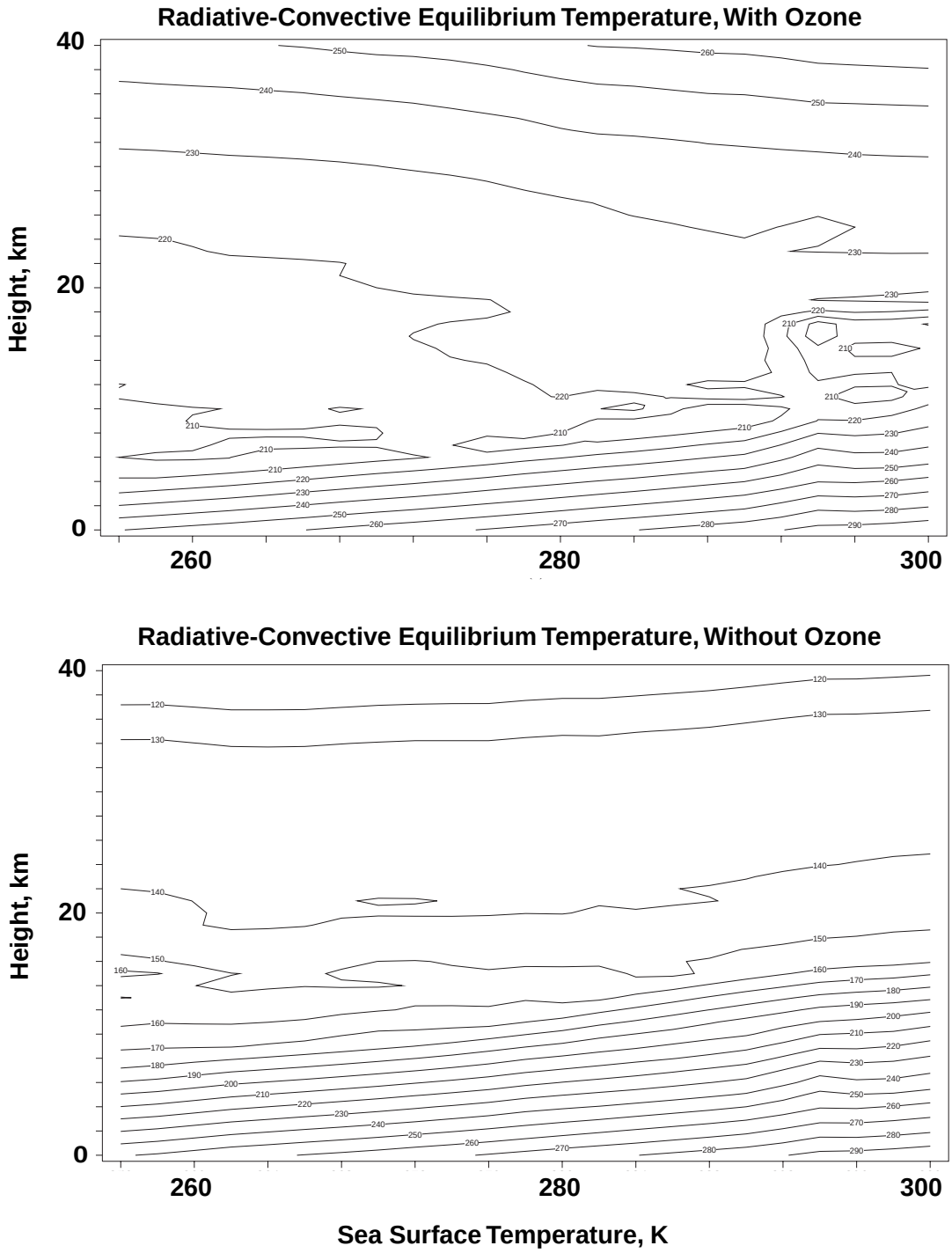

Figure 6.4: **Temperature profiles for radiative - convective equilibrium, as simulated by the physical parameterizations of the CSU GCM. The surface temperature was prescribed as a more or less realistic function of latitude, and for each latitude the annual mean insolation was used.**

structure of the stratosphere and mesosphere, which are often referred to as the "middle atmosphere." Because the middle atmosphere has a very stable stratification, convection is not active there. The results obtained by Fels are shown in Fig. 6.5. The observed state of the

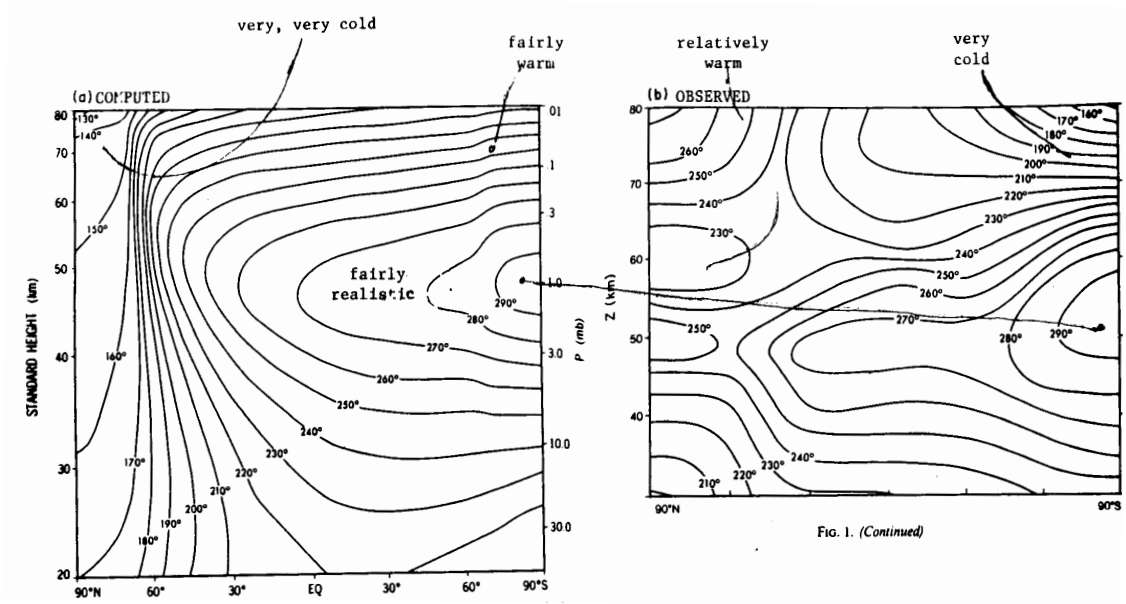

FIG. 1. *(Continued)*

Figure 6.5: **(a) Zonal mean temperatures for 15 January calculated by using a time-marched radiative-convective-photochemical model. (b) Zonal mean temperatures for January. From Fels (1985).**

atmosphere (see panel b of Fig. 6.5) resembles that predicted by the model in the summer stratosphere, but the model is much too cold in the winter polar stratosphere. Also, the mesosphere of the real world is warm near the winter pole and cold near the summer pole, while the model predicts just the opposite. The differences between the observations and the model results can be attributed to the effects of large-scale motions, which are neglected in the model. Obviously, the motions make quite a difference in the winter middle atmosphere, where they must transport energy poleward in order to account for the differences between the observations and the results of the radiative-convective model. It appears that large-scale motions have little effect on the thermal structure of the middle atmosphere in summer, however. This indicates that in the summer the middle atmosphere is close to a state of radiative equilibrium.

6.3 The observed vertical structure of the atmosphere, and the mechanisms of vertical energy transport

Fig. 6.6 shows the observed vertical structure of the atmosphere in the tropics, the subtropical tradewind regime, and the subtropical marine stratocumulus regime. The quantities plotted are the dry static energy, defined by

$$s \equiv c_p T + gz \,, \tag{6.19}$$

the moist static energy, defined by

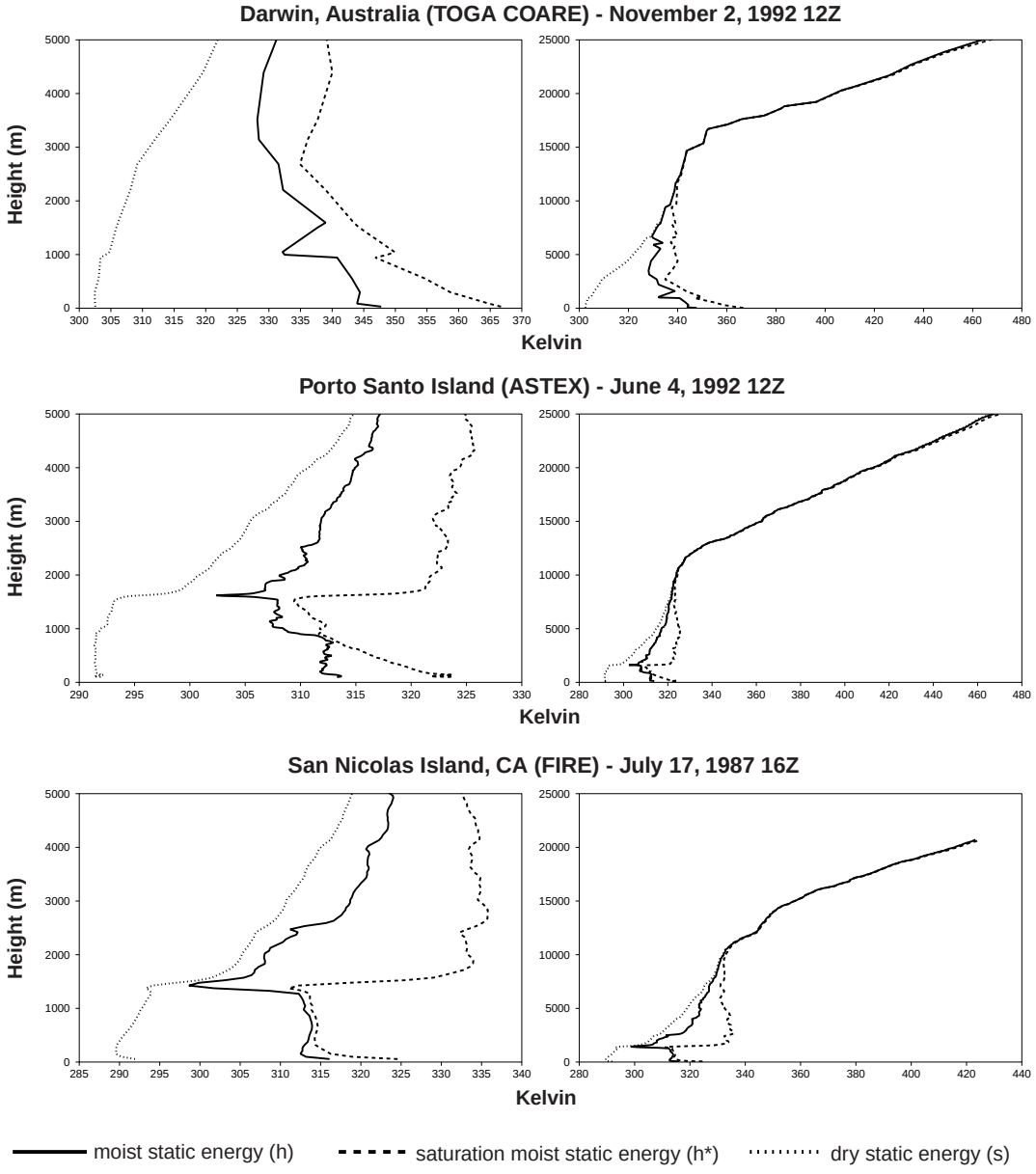

Figure 6.6: **Representative observed soundings for Darwin, Australia, Porto Santo Island in the Atlantic tradewind regime, and San Nicolas Island, in the subtropical marine stratocumulus regime off the coast of southern California. The curves plotted show the dry static energy, the moist static energy, and the saturation moist static energy. The panels on the right cover both the troposphere and lower stratosphere, while those on the right zoom in on the lower troposphere to show more detail. Values are divided by c_p to give units in K.**

$$h \equiv s + Lq_v, \tag{6.20}$$

and the saturation moist static energy, defined by

$$h^* \equiv s + Lq^*. \tag{6.21}$$

Here q^* is the saturation mixing ratio. At cold temperatures, these three quantities are nearly equal, because both the water vapor mixing ratio and the saturation mixing ratio are small. Quite generally, we have

$$s \le h \le h^*. \tag{6.22}$$

In cloudy air, $h = h^*$. In very dry air, $h \cong s$. In very cold air, $h^* \cong h \cong s$. It can be shown that the dry static energy increases upward in a statically stable atmosphere. The dry static energy is approximately conserved under dry adiabatic processes, while the moist static energy is approximately conserved under dry adiabatic, moist adiabatic, and pseudo-adiabatic processes. The saturation moist static energy is not a conservative variable, and despite its name it does not actually carry any information about the moisture field; the sounding of the saturation moist static energy is essentially determined by the temperature sounding.

If a parcel of air containing vapor is lifted adiabatically from near the surface, it will eventually become saturated due to the cooling caused by adiabatic expansion. Prior to reaching its lifting condensation level, both the dry static energy and the moist static energy of the parcel will be conserved. Once the lifting condensation level has been exceeded, the moist static energy of the now-cloudy parcel will continue to remain constant, while its dry static energy will increase upward due to latent heat release. The liquid water mixing ratio will increase, and the water vapor mixing ratio will correspondingly decrease. Under moist adiabatic processes, the total mixing ratio, $q_v + l$, will be conserved.

Note that conservation of h and $q_v + l$ implies that

$$s_l \equiv h - L(q_v + l) \tag{6.23}$$

is also conserved. We refer to s_l as the "liquid water static energy." It is conserved under moist adiabatic processes. Precipitation from a parcel is not a moist adiabatic process, because it involves the removal of mass from the parcel. Precipitation can change the value of s_l, but it does not change the value of h. This means that h is "more conservative" than s_l. Nevertheless both variables are useful.

The temperature difference between the cloudy air and its environment at the same level is simply proportional to the saturation moist static energy difference, i.e.

$$c_p(T_c - \bar{T}) \sim h^*_c - \overline{h^*}\ , \tag{6.24}$$

where a subscript *c* denotes the cloudy air, and an overbar denotes the environment. Because the cloudy air is saturated, however, we can write

$$c_p(T_c - \bar{T}) \sim h_c - \overline{h^*} \ . \tag{6.25}$$

This shows that the buoyancy of the cloudy air, as measured by the difference between its temperature and the temperature of the environment, is proportional to the difference between the moist static energy of the cloudy air and the saturation moist static energy of the environment. Recall, however, that we are considering a parcel that is lifted adiabatically from near the surface, conserving its moist static energy. This means that h_c is equal to the low-level moist static energy of the sounding. The cloudy updraft will stop when it encounters a level where $h_c = \overline{h^*}$; if this level is high and cold, then $\overline{h^*} \cong \bar{h}$, and so we expect to find

$$h_{\text{tropopause}} \cong h_{\text{boundary layer}} \text{ in regions where deep convection is active.} \tag{6.26}$$

In the terminology of Neelin and Held (1987), Eq. (6.29) means that the gross moist stability is small. See (6.8).

We can apply these ideas to the tropical (i.e. Darwin) sounding shown in Fig. 6.6. Near the surface, $h^* > h$, indicating that the air is unsaturated. If we lift a parcel adiabatically from near the surface, its moist static energy will follow a straight, vertical line in the diagram, starting from a near-surface value. At the same time, the environmental saturation moist static energy decreases upward. After rising a kilometer or so, the vertical line representing the moist static energy traced out by adiabatic parcel ascent from the surface will be to the right of the observed sounding of saturation moist static energy, so that $h_c > \overline{h^*}$. According to (6.25), the parcel will then be positively buoyant, *if it is saturated*. We can thus tell, simply by looking at Fig. 6.6, that the Darwin sounding is conditionally unstable. The positive buoyancy of the lifted parcel will continue upward until the vertical line representing constant moist static energy again crosses over to the left side of the curve representing the environmental saturation moist static energy. For the Darwin soundings, this occurs at about the 15 km level, near the tropopause. We thus expect deep cumulus convection to occur in this sounding, although the mere existence of a conditionally unstable sounding is not enough, in itself, to show that cumulus convection will be significantly active.

The subtropical "tradewind" sounding is also conditionally unstable, but only through a shallow layer. The tradewind convective layer is capped by a very strong temperature inversion, and the water-vapor mixing ratio decreases strongly upward through this "trade inversion." The middle troposphere is much drier in the tradewind sounding than in the tropical sounding.

The subtropical marine stratocumulus sounding is not conditionally unstable at all. The sounding shows evidence of cloudiness in the lowest kilometer. The cloud layer is capped by a very strong inversion, essentially similar to the trade inversion, but residing at a lower level. Marine stratocumulus regimes occur in several places around the world, typically in association with subtropical highs. See Fig. 6.7.

The physical picture represented by the three soundings shown in Fig. 6.6 is

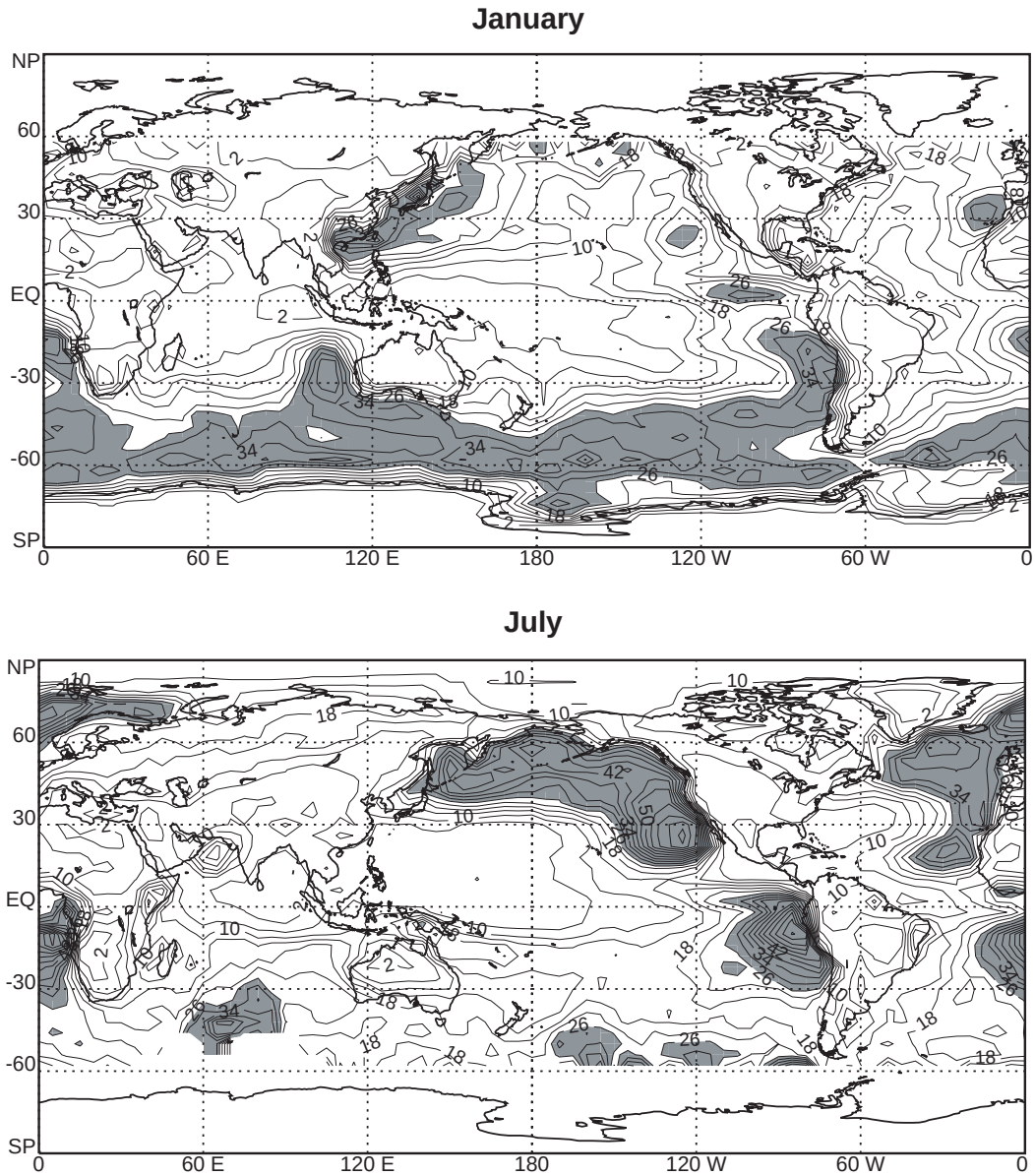

Figure 6.7: **Observed locations of low-level stratus clouds, including the one west of California , as observed by ISCCP, the International Satellite Cloud Climatology Project. Cloud amounts higher than 26% are shaded.**

summarized in Fig. 6.8. The subtropical marine stratocumulus regime is shown on the right side of the figure, in a region of large-scale subsidence. The sea surface temperatures are relatively cool in such regimes. Towards the left, we enter the tradewind cumulus regime, which has weaker subsidence and warmer sea surface temperatures. Finally on the left side of the figure we reach the region of deep convection, characterized by warm sea surface temperatures and large-scale rising motion.

As the air descends in the subtropical branches of the Hadley cells, it is gradually

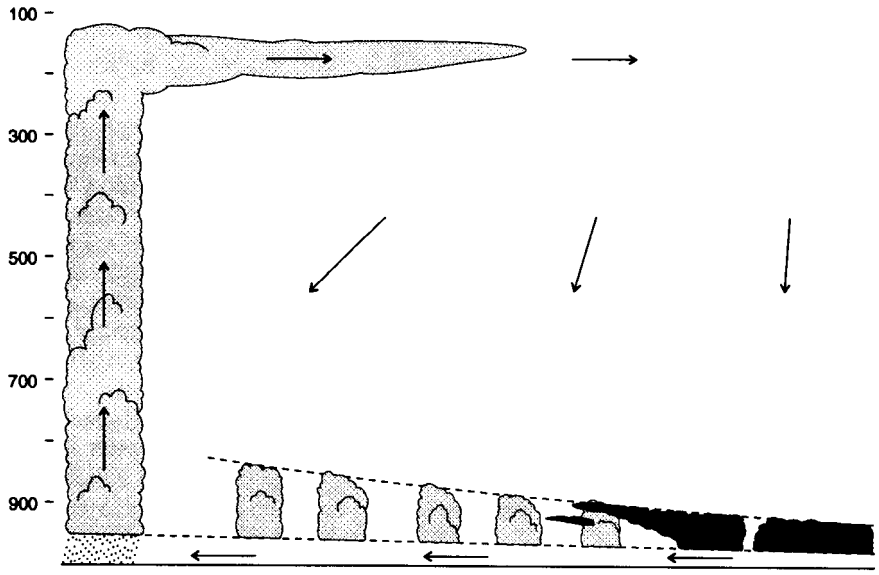

Figure 6.8: Schematic diagram summarizing the relationships among the cloud regimes depicted in Fig. 6.6, and how they fit into the mean meridional circulation. From Schubert et al. (1995).

cooled by radiation. As a result, the potential temperature of the air in the subtropical free atmosphere decreases downward, or in other words it increases upward.

The lapse rate of the deep convective zones is essentially determined by convection. As already noted, however, the horizontal temperature gradients are weak throughout the tropics and subtropics, for reasons discussed by Charney (1963). This means that the lapse rate in the subtropics, above the trade inversion, must be nearly the same as the lapse rate in the tropics. We can write a rough thermodynamic balance for the descending branch of the Hadley cell as follows:

$$\omega \frac{\partial s}{\partial p} = Q_R . \tag{6.27}$$

Here ω is the positive large-scale pressure velocity, corresponding to sinking motion; $\frac{\partial s}{\partial p}$ is the rate of change of the dry static energy with height, which we have just argued is essentially imposed, above the trade inversion, by the moist convective processes of the deep tropics; and $Q_R < 0$ is the radiative cooling. We see from (6.27) that the speed of the large-scale sinking motion in the subtropics is essentially determined by the requirement of thermodynamic balance. Typical clear-sky tropospheric radiative cooling rates in the tropics are on the order of 2 K per day (Fig. 6.9).

The sinking air passes through the trade inversion. How does this happen? It is remarkable, for example, that the average mixing ratio of the air suddenly increases from perhaps 1 g kg^{-1} above the trade inversion to 6 or 7 g kg^{-1} below the trade inversion. This is the

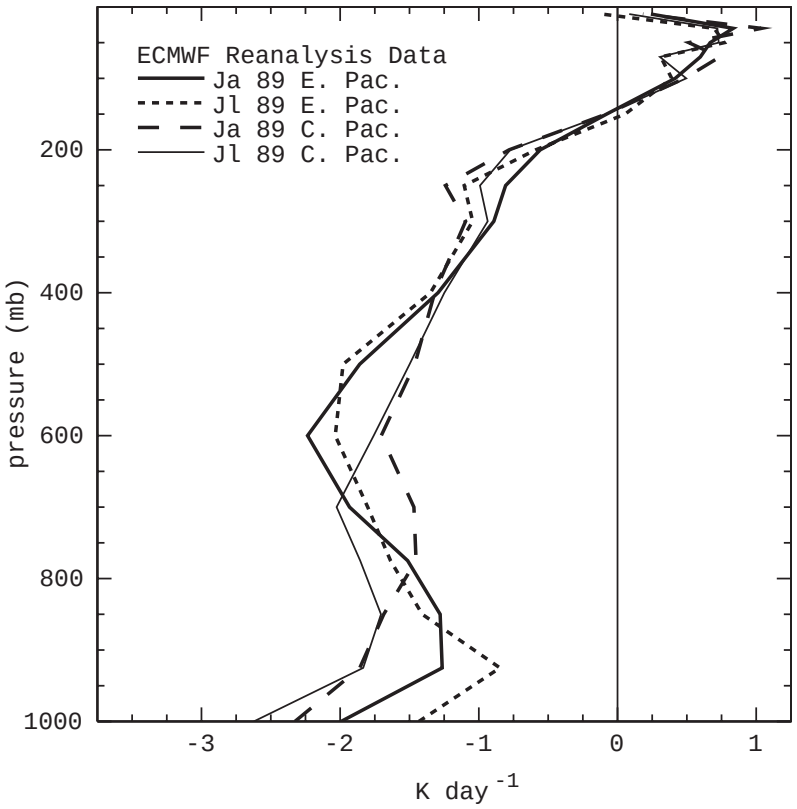

Figure 6.9: **Estimates of the clear-sky radiative cooling rate in the eastern and central Pacific, based on ECMWF data.**

same air, after all; how does it suddenly become so moist? The answer is that the convective vertical motions associated with the shallow stratocumulus and/or trade cumulus clouds transport moisture upwards, and deposit it at the base of the inversion, where it is used to moisten the sinking air. The moisture used for this purpose is carried up from the sea surface by a combination of turbulence and shallow cloudy convection.

The air also cools as it descends through the inversion. This cooling is produced by a combination of concentrated radiative cooling near cloud tops, evaporative cooling due to the evaporation of liquid deposited at the trade inversion level by the shallow clouds, and a downward flux of sensible heat that cools the air as it crosses the inversion.

A macroscopic view of this entrainment process is as follows. Let A be an arbitrary scalar, satisfying a conservation equation that can be written in "flux form" as

$$\frac{\partial}{\partial t}(\rho A) + \nabla \bullet (\rho \mathbf{V} A) + \frac{\partial}{\partial z}(\rho w A) = -\frac{\partial F_A}{\partial z} + S_A , \tag{6.28}$$

where $F_A \equiv \rho \overline{w' A'}$ is the upward turbulent flux of A, bars are omitted on the mean

quantities, and S_A is a source or sink of A, per unit volume. Integrating (6.28) from just below to just above the inversion, and using Leibniz' rule, we get

$$\frac{\partial}{\partial t}\int_{z_B-\varepsilon}^{z_B+\varepsilon}\rho A\,dz - \Delta(\rho A)\frac{\partial z_B}{\partial t} + \nabla\bullet\int_{z_B-\varepsilon}^{z_B+\varepsilon}\rho\mathbf{V}A\,dz - \Delta(\rho\mathbf{V}A)\bullet\nabla z_B + \Delta(\rho wA) = -(F_A)_{B+} + (F_A)_B + \int_{z_B-\varepsilon}^{z_B+\varepsilon} S_A\,dz\,, \tag{6.29}$$

where the indicated terms drop out as the domain of integration shrinks to zero and/or because all of the turbulence variables go to zero above the inversion. Here we have used the notation $\Delta(\ ) \equiv (\ )_{z=z_B+\varepsilon} - (\ )_{z=z_B-\varepsilon} \equiv (\ )_{B+} - (\ )_B$, and henceforth subscripts B+ and B denote levels just above and just below the inversion, respectively. For $A \equiv 1$, (6.29) reduces to mass conservation in the form

$$\rho_{B+}\left(\frac{\partial z_B}{\partial t} + \mathbf{V}_{B+}\bullet\nabla z_B - w_{B+}\right) = \rho_B\left(\frac{\partial z_B}{\partial t} + \mathbf{V}_B\bullet\nabla z_B - w_B\right) = E\,, \tag{6.30}$$

where E is the downward mass flux across the inversion. In essence, (6.30) simply says that the mass flux is continuous across the PBL top, i.e. no mass is created or destroyed between levels B and B+. We interpret E as the mass flux due to the turbulent *entrainment* of free atmospheric air across the inversion. With the definition of E as given by (6.30), we can rewrite (6.29) as

$$-\Delta AE = (F_A)_B + \int_{z_B-\varepsilon}^{z_B+\varepsilon} S_A\,dz\,, \tag{6.31}$$

For $S_A \equiv 0$, (6.31) simply says that the total flux of A must be continuous across the inversion. Notice that for $\Delta A \neq 0$, a mass flux across the inversion is generally associated with the convergence of a turbulent flux of A at level B. This flux convergence changes the A of entering particles from A_{B+} to A_B. Lilly (1968; Fig. 6.10) was the first to derive (6.31) using the approach followed here.

As a simple example, consider the moistening of the air as it moves down across the inversion. The dry entrained air is moistened by an upward moisture flux that converges "discontinuously" at level B. This is described by

$$-\Delta q_T E = (F_{q_T})_B\,, \tag{6.32}$$

Figure 6.10: Douglas Lilly, who has done leading work on a wide range of topics including cumulus convection, numerical methods, gravity waves, and stratocumulus clouds.

which is a special case of (6.31). Here $q_T \equiv q_v + l$ is the total water mixing ratio.

After sinking through the trade inversion, the air is subjected to friction. This causes its angular momentum to decrease. As it flows back equatorward, near-surface easterlies result.

Turning now to middle and high latitudes, Fig. 6.6 shows representative summer and winter soundings for Denver, Colorado and Barrow, Alaska. The Denver sounding is conditionally unstable in summer, but the dry near-surface air has to be lifted quite a long way before it can become positively buoyant; we expect to see high cloud bases. The winter sounding for Denver is strongly stable near the surface. The Barrow sounding is quite stable all year, but especially so in winter. Note that the tropopause is much lower at Barrow that at Darwin. In summer, there are low clouds at Barrow.

6.4 More on moist convection

The preceding discussion suggests that moist convection is important in two ways:

- As shown observationally by Riehl and Malkus (1958), moist convection is the primary mechanism to transport energy upward in the deep tropics. Convection also transports moisture and momentum, as well as various chemical constituents.
- As hypothesized by Manabe and Wetherald (1967), convection acts to prevent the lapse rate *in convectively active regions* from exceeding a value close to the moist adiabatic lapse rate. Even if we accept the validity of this hypothesis, we are faced with the problem of determining when and where convection is active.

In addition, of course, moist convection is important because:

- Convection produces a large fraction of the Earth's precipitation.
- Convection generates radiatively important stratiform clouds, especially in the upper troposphere in regions of deep convection.

For the four reasons summarized in the four bullets above, *moist convection is crucially*

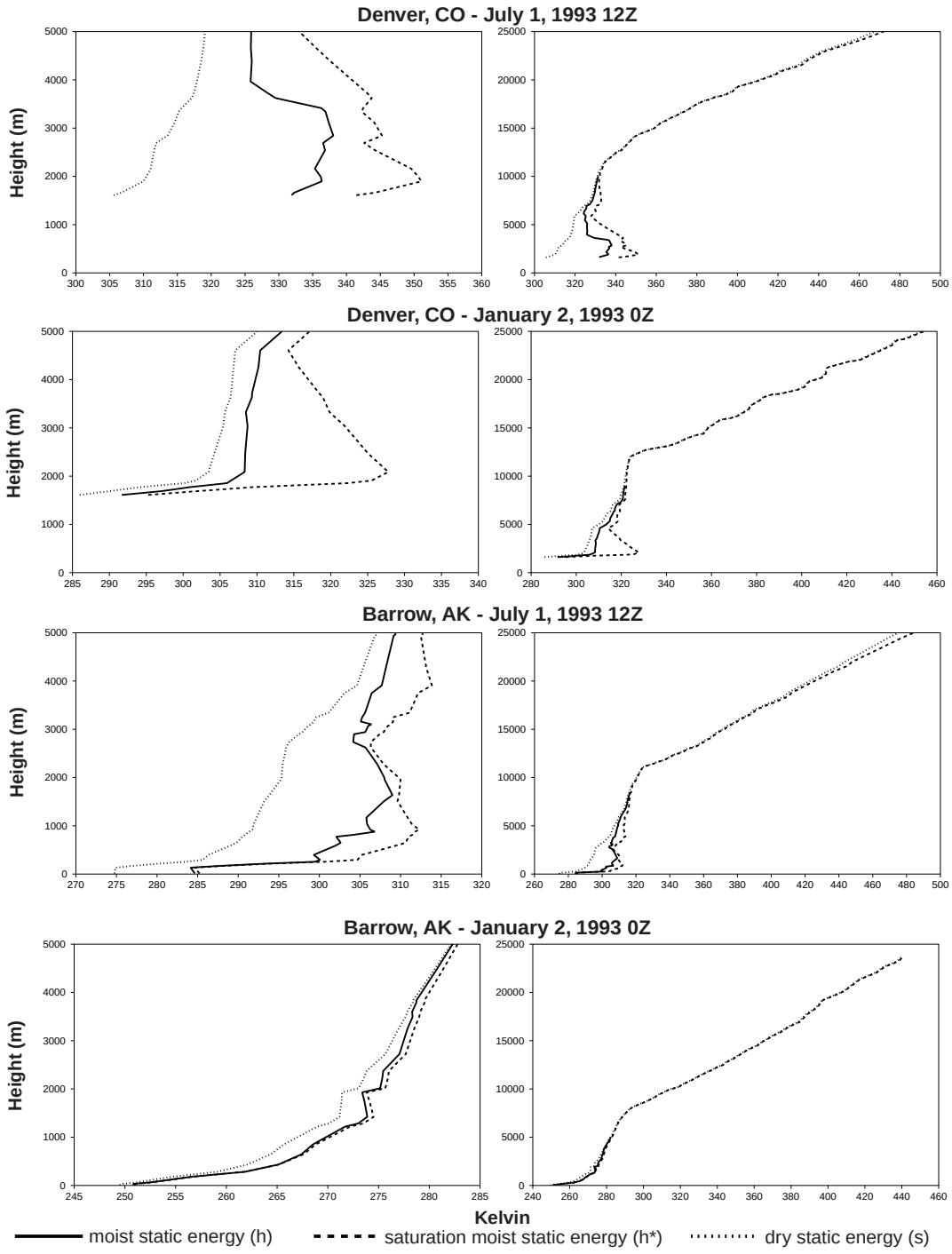

Figure 6.11: **Representative observed soundings for Denver, Colorado and Barrow, Alaska, for July and January. The curves plotted show the dry static energy, the moist static energy, and the saturation moist static energy. The panels on the right cover both the troposphere and lower stratosphere, while those on the right zoom in on the lower troposphere to show more detail. Values are divided by c_p to give units in K.**

important for the general circulation of the Earth's atmosphere. It is no exaggeration to say that we cannot understand the general circulation unless we understand the interactions between the general circulation and moist convection. In fact there is an enormous literature on this subject of "cumulus parameterization," and many contentious issues remain unresolved, while many additional issues have not even been confronted yet. Current ideas are that cumulus convection exerts its effects on the large-scale stratification by transporting mass vertically (the so-called "cumulus mass flux"), and that the intensity of convection is regulated by the processes that act to produce convective instability; these include radiative cooling of the air relative to the temperature of the lower boundary, surface fluxes of sensible and latent heat, and the effects of both horizontal and vertical advection, including moisture convergence from neighboring columns.

The effects of convection on the large-scale state can be analyzed following Arakawa and Schubert (1974; hereafter AS; see Fig. 6.12). Let an overbar denote a suitable average.

Figure 6.12: **Prof. Akio Arakawa, cruising along in mid-lecture.**

The averaged budget equations for mass, dry static energy, water vapor mixing ratio, and liquid water mixing ratio are:

$$0 = -\nabla \bullet (\overline{\rho \mathbf{V}}) - \frac{\partial}{\partial z}(\overline{\rho w}), \tag{6.33}$$

$$\overline{\rho}\frac{\partial \bar{s}}{\partial t} = -\overline{\rho}\overline{\mathbf{V}} \bullet \nabla \bar{s} - \overline{\rho w}\frac{\partial \bar{s}}{\partial z} + \overline{Q_R} L\bar{C} - \frac{\partial F_s}{\partial z}, \tag{6.34}$$

$$\overline{\rho}\frac{\partial \overline{q_v}}{\partial t} = -\overline{\rho}\overline{\mathbf{V}} \bullet \nabla \overline{q_v} - \overline{\rho w}\frac{\partial \overline{q_v}}{\partial z} - \bar{C} - \frac{\partial F_{q_v}}{\partial z}, \tag{6.35}$$

$$\rho\frac{\partial \bar{l}}{\partial t} = -\rho\bar{\mathbf{V}}\bullet\nabla\bar{l} - \rho\bar{w}\frac{\partial \bar{l}}{\partial z} + \bar{C} - \frac{\partial F_l}{\partial z} - \bar{\chi}\,. \tag{6.36}$$

Here ρ is the density of the air, which is presumed to be quasi-constant at each height[2]; $s \equiv c_p T + gz$ is the dry static energy; T is temperature; c_p is the specific heat at constant pressure; q is the water vapor mixing ratio; w is the vertical velocity; $\bar{\mathbf{V}}$ is the horizontal velocity; L is the latent heat of evaporation; *C is the net rate of condensation,* Q_R is the radiative heating rate, and χ is the rate at which liquid water is being converted into precipitation, which then falls out and so acts as a sink of l. The vertical "eddy fluxes," $F_s \equiv \rho\overline{ws} - \rho\bar{w}\bar{s}$ and $F_{q_v} \equiv \rho\overline{wq_v} - \rho\bar{w}\bar{q}_v$, can in principle represent quite a variety of physical processes, but here we assume for simplicity that above the boundary layer these fluxes are due only to the vertical currents associated with cumulus convection. Compare (6.34) with (6.9).

AS used a very simple cumulus cloud model to formulate the eddy fluxes that appear in (6.34) and (6.35) in terms of a convective mass flux and the differences between the in-cloud and environmental soundings. The cloud model was also used to formulate the net condensation rate, C, per unit mass flux. AS allowed the possibility that clouds of many different "types" coexist; here a cloud type can be roughly interpreted as a cloud size category. We now briefly explain the AS parameterization, using a single cloud type for simplicity.

As a first step, we divide the domain into an arbitrary number N of subdomains, each having a characteristic fractional area σ_i, a characteristic vertical velocity w_i, and corresponding characteristic values of the moist static energy, dry static energy, water vapor mixing ratio, and all of the other variables of interest. Some of the subdomains represent cloudy updrafts or downdrafts, while others could represent mesoscale subdomains or the broad "environment" of the clouds. The fractional areas must sum to unity:

$$\sum_{i=1}^{N} \sigma_i = 1\,. \tag{6.37}$$

The area-averaged vertical velocity and moist static energy satisfy:

$$\sum_{i=1}^{N} \sigma_i w_i = \bar{w}, \tag{6.38}$$

[2] This is the "anelastic" approximation. A handout on this topic is available from the instructor. Because the density is assumed to be quasi-constant at each height, we do not bother to put an over-bar on it.

$$\sum_{i=1}^{N} \sigma_i h_i = \bar{h} \,. \tag{6.39}$$

It then follows algebraically that

$$F_h \equiv \rho\overline{wh} - \rho\bar{w}\bar{h} = \sum_{i=1}^{N} \rho\sigma_i (w_i - \bar{w})(h_i - \bar{h}) \,. \tag{6.40}$$

You should work through the derivation to satisfy yourself that this is true.

We now assume for simplicity that mesoscale organization and convective-scale downdrafts are not significant, so that the cloudy layer consists of concentrated convective updrafts of various sizes and intensities, embedded in a broad uniform environment. We use a superscript tilda to denote an environmental value, and a subscript c to denote the collective properties of the cloudy updrafts. Then (6.37) can be rewritten as

$$\sigma_c + \tilde{\sigma} = 1 \,. \tag{6.41}$$

Here

$$\sigma_c \equiv \sum_{\text{all clouds}} \sigma_i \tag{6.42}$$

is the total fractional area covered by all of the convective updrafts, and $\tilde{\sigma}$ is the fractional area of the environment. Similarly, (6.38) and (6.39) become

$$\sigma_c w_c + \tilde{\sigma} w = w \,, \tag{6.43}$$

$$\sigma_c h_c + \tilde{\sigma} h = \bar{h} \,, \tag{6.44}$$

where we define

$$w_c \equiv \frac{\sum_{\text{all clouds}} \sigma_i w_i}{\sigma_c} \,, \tag{6.45}$$

$$h_c \equiv \frac{\sum_{\text{all clouds}} \sigma_i h_i}{\sigma_c} \,. \tag{6.46}$$

It is observed that

$$\sigma_c \ll 1 \text{, and } \tilde{\sigma} \cong 1 . \tag{6.47}$$

This means that the cumulus updrafts occupy only a very small fraction of the area. A simple explanation for this important fact was given by Bjerknes (1938). Suppose that at a certain time the temperature is horizontally uniform, with lapse rate

$$\Gamma \equiv -\frac{\partial T}{\partial z} . \tag{6.48}$$

In a cloudy region, the temperature satisfies

$$\frac{\partial T_c}{\partial t} = w_c(\Gamma - \Gamma_m) . \tag{6.49}$$

In a neighboring clear region,

$$\frac{\partial}{\partial t}\tilde{T} = \tilde{w}(\Gamma - \Gamma_d) . \tag{6.50}$$

The mean vertical motion satisfies (6.43), from which it follows that

$$w_c = \bar{w} + (1 - \sigma_c)(w_c - \tilde{w}) , \tag{6.51}$$

$$\tilde{w} = \bar{w} - \sigma_c(w_c - \tilde{w}) . \tag{6.52}$$

Substituting, we find that

$$\begin{aligned} \frac{\partial}{\partial t}(T_c - \tilde{T}) &= w_c(\Gamma - \Gamma_m) - \tilde{w}(\Gamma - \Gamma_d) \\ &= \bar{w}(\Gamma_d - \Gamma_m) + (w_c - \tilde{w})[(1 - \sigma_c)(\Gamma - \Gamma_m) + \sigma_c(\Gamma - \Gamma_d)]. \end{aligned} \tag{6.53}$$

If the sounding is conditionally unstable, then

$$\Gamma - \Gamma_m > 0 \text{ and } \Gamma - \Gamma_d < 0 . \tag{6.54}$$

We can therefore conclude from (6.53) that $T_c - \tilde{T}$ will increase most rapidly if $\sigma_c \to 0$. The physical interpretation is simple. With a conditionally unstable sounding, saturated rising motion is aided by positive buoyancy created through condensation, while unsaturated sinking motion must fight against the dry-stable stratification. The rate at which the updraft gains buoyancy is proportional to the updraft speed, while the rate at which the downdraft must fight against the stratification is proportional to the downdraft speed. Therefore, the convection is favored by rapid rising motion in the cloudy region, and slow sinking motion in the clear

region, both of which can be achieved, for a given value of $w_c - \tilde{w}$, by making the updraft narrow, and the downdraft broad.

In view of (6.47), we can write (6.44) as

$$\tilde{h} \cong \bar{h}, \tag{6.55}$$

It is *not* true, however, that $\tilde{w} \cong \bar{w}$, because the cumulus updrafts are typically several orders of magnitude stronger than the large-scale vertical motions:

$$\sum_{\text{all clouds}} \sigma_i w_i \gg \bar{w}. \tag{6.56}$$

Similarly, it is not true in general that $\bar{l} \cong \tilde{l}$, because there may be no liquid water at all in the environment of the convective clouds.

Using (6.56), we can approximate (6.40) by

$$F_h \cong \sum_{i=1}^{N} M_i (h_i - \bar{h}) \tag{6.57}$$

where

$$M_i \equiv \rho \sigma_i w_i \tag{6.58}$$

is the "convective mass flux" associated with cloud type i. *The convective mass flux is a key concept.* It represents the rate at which mass is pumped through the convective circulations -- through the updraft, through the compensating sinking motion outside the updraft, and through the horizontal branches of the convective circulation that connect the updraft and the sinking motion.

From this point we simplify the discussion by considering only one type of convective cloud, whose properties are denoted by subscript c. We write

$$F_s \cong M_c (s_c - \bar{s}), \tag{6.59}$$

$$F_{q_v} \cong M_c [(q_v)_c - \overline{q_v}], \tag{6.60}$$

$$F_l \cong M_c (l_c - \bar{l}). \tag{6.61}$$

Here s_c, $(q_v)_c$, and l_c are the in-cloud dry static energy, water vapor mixing ratio, and liquid water mixing ratio, respectively, and

$$M_c \equiv \rho \sigma_c w_c . \tag{6.62}$$

Note that we allow the possibility of liquid water in the environment of the cumulus clouds. We also use

$$\bar{s} = (1-\sigma_c)\tilde{s} + \sigma_c s_c , \tag{6.63}$$

$$\overline{q_v} = (1-\sigma_c)\tilde{q_v} + \sigma_c (q_v)_c , \tag{6.64}$$

$$\bar{l} = (1-\sigma_c)\tilde{l} + \sigma_c l_c , \tag{6.65}$$

$$\overline{C} = (1-\sigma_c)\tilde{C} + \sigma_c C_c , \tag{6.66}$$

$$\bar{\chi} = (1-\sigma_c)\tilde{\chi} + \sigma_c \chi_c . \tag{6.67}$$

We can now rewrite (6.34) - (6.36) as

$$\rho \frac{\partial \bar{s}}{\partial t} = -\rho \overline{\mathbf{V}} \bullet \nabla \bar{s} - \rho \overline{w} \frac{\partial \bar{s}}{\partial z} + \overline{Q_R} L(\tilde{C} + \sigma_c C_c) - \frac{\partial}{\partial z}[M_c(s_c - \bar{s})] , \tag{6.68}$$

$$\rho \frac{\partial \overline{q_v}}{\partial t} = -\rho \overline{\mathbf{V}} \bullet \nabla \overline{q_v} - \rho \overline{w} \frac{\partial \overline{q_v}}{\partial z} - (\tilde{C} + \sigma_c C_c) - \frac{\partial}{\partial z}\{M_c[(q_v)_c - \overline{q_v}]\} , \tag{6.69}$$

$$\rho \frac{\partial \bar{l}}{\partial t} = -\rho \overline{\mathbf{V}} \bullet \nabla \bar{l} - \rho \overline{w} \frac{\partial \bar{l}}{\partial z} + (\tilde{C} + \sigma_c C_c) - \frac{\partial}{\partial z}[M_c(l_c - \bar{l})] - [(1-\sigma_c)\tilde{\chi} + \sigma_c \chi_c] . \tag{6.70}$$

Eq. (6.47) has been used here. Note that the convective condensation rate, C_c, appears in all three of these equations, as would be expected.

To go further we need to describe what is going on inside the convective updrafts; for example, we need to know the soundings in side the updrafts. We assume that all cumulus clouds originate from the top of the PBL, carrying the mixed-layer properties upward. The mass flux changes with height according to

$$\frac{\partial}{\partial z} M_c(z) = E(z) - D(z) . \tag{6.71}$$

Here E is the entrainment rate, and D is the detrainment rate. The in-cloud profile of moist

static energy, $h_c(z)$, is governed by

$$\frac{\partial}{\partial z}[M_c(z)h_c(\lambda, z)] = E(z)\bar{h}(z) - D(z)h_c(z) \ . \tag{6.72}$$

There are no source or sink terms in this equation because the moist static energy is unaffected by phase changes and/or precipitation processes.[3] By combining (6.71) and (6.72), we can obtain

$$\frac{\partial}{\partial z}h_c(z) = \frac{E(z)}{M_c}[\bar{h}(z) - h_c(z)] \, . \tag{6.73}$$

This shows that $h_c(z)$ is affected by entrainment, which dilutes the cloud with environmental air, but not by detrainment, which has been assumed to expel from the cloud air that has the average moist static energy of the cloud at each level. Similarly, we can write

$$\frac{\partial}{\partial z}(M_c s_c) = E\bar{s} - Ds_c + \sigma_c L C_c \, , \tag{6.74}$$

$$\frac{\partial}{\partial z}[M_c(q_v)_c] = E\overline{q_v} - D(q_v)_c - \sigma_c C_c \, , \tag{6.75}$$

$$\frac{\partial}{\partial z}(M_c l_c) = E\bar{l} - Dl_c + \sigma_c C_c - \chi_c \, . \tag{6.76}$$

A simple microphysical model is used to determine χ_c, i.e. to determine how much of the condensed water is converted to precipitation, and the fate of the precipitation. The role of convectively generated precipitation, which drives convective downdrafts and moistens the lower troposphere by evaporating as it falls, is actually an important and currently active topic in the arena of cumulus parameterization, but it will not be discussed here.

By using these expressions for the convective fluxes, the large-scale budget equations can be rewritten in a very interesting form, as follows. First, consider the dry static energy. We write

$$-\frac{\partial}{\partial z}[M_c(s_c - \bar{s})] = -\frac{\partial}{\partial z}(M_c s_c) + M_c\frac{\partial}{\partial z}\bar{s} + \bar{s}\frac{\partial M_c}{\partial z} \, . \tag{6.77}$$

Now substitute from (6.74) and (6.77) into (6.80) to obtain

[3] Radiation effects on the in-cloud moist static energy are neglected here.

$$-\frac{\partial}{\partial z}[M_c(s_c-\bar{s})] = -(E\bar{s}-Ds_c+L\sigma_c C_c)+M_c\frac{\partial \bar{s}}{\partial z}+\bar{s}(E-D)$$
$$= M_c\frac{\partial \bar{s}}{\partial z}+D(s_c-\bar{s})-L\sigma_c C_c\ . \tag{6.78}$$

This allows us to rewrite (6.68) as

$$\rho\frac{\partial \bar{s}}{\partial t} = -\rho\bar{\mathbf{V}}\bullet\nabla\bar{s}-\rho\bar{w}\frac{\partial \bar{s}}{\partial z}+\overline{Q_R}+L\tilde{C}+M_c\frac{\partial \bar{s}}{\partial z}+D(s_c-\bar{s})\ . \tag{6.79}$$

The last two terms on the right-hand side of (6.79) represent the cumulus effects, and the first of these in particular is quite interesting. It "looks like" an advection term. *It represents the warming of the environment due to the downward advection of air from above, with higher dry static energies, by the environmental sinking motion that compensates for the rising motion in the cloudy updraft. The environmental sinking motion is called "compensating subsidence."* The effect can be seen more explicitly by combining the two "vertical advection" terms of (6.79), and using (6.81), to obtain

$$\rho\frac{\partial \bar{s}}{\partial t} = -\rho\bar{\mathbf{V}}\bullet\nabla\bar{s}-\tilde{M}\frac{\partial \bar{s}}{\partial z}+\overline{Q_R}+L\tilde{C}+D(s_c-\bar{s})\ . \tag{6.80}$$

$$\tilde{M}\equiv\rho\bar{w}-M_c\ , \tag{6.81}$$

The reason that M appears in (6.81) is that (6.55) applies, i.e. $s = s$. The last term on the right-hand side of (6.79) represents the effects of detrainment. Notice that the cumulus condensation rate does not appear in (6.79). An interpretation is that condensation inside the updraft cannot directly warm the environment, and since almost the entire area is the environment, this means that condensation does not, to any significant degree, *directly* affect the area-averaged value of the dry static energy. Instead, the effects of condensation are felt *indirectly*, through the compensating subsidence term, which we have already interpreted. The physical role of condensation, then, is to make possible the convective updraft that drives the compensating subsidence, which in turn warms the environment. This is how condensation warms indirectly. Note that the vertical profile of the indirect condensation heating rate due to compensating subsidence is in general different from the vertical profile of the convective condensation rate itself.

In a similar way, we find by analogy with (6.79) that the water vapor and liquid water budget equations can be rewritten as

$$\rho\frac{\partial \bar{q}_v}{\partial t} = -\rho\bar{\mathbf{V}}\bullet\nabla\bar{q}_v-\rho\bar{w}\frac{\partial \bar{q}_v}{\partial z}-\tilde{C}+M_c\frac{\partial \bar{q}_v}{\partial z}+D[(q_v)_c-\bar{q}_v]\ , \tag{6.82}$$

$$\rho\frac{\partial \bar{l}}{\partial t} = -\rho\bar{\mathbf{V}}\bullet\nabla\bar{l}-\rho\bar{w}\frac{\partial \bar{l}}{\partial z}+\tilde{C}+M_c\frac{\partial \bar{l}}{\partial z}+D(l_c-\bar{l})-[(1-\sigma_c)\tilde{\chi}+\sigma_c\chi_c]\ . \tag{6.83}$$

Eq. (6.82) describes the convective drying in terms of convectively-induced subsidence in the environment, which brings down drier air from aloft. Detrainment of water vapor from the convective clouds can moisten the environment. Detrained liquid (or ice) can persist in the form of stratiform "anvil" and cirrus clouds.

Within the limits of applicability of the assumptions discussed above, (6.79) and (6.82) - (6.82) are equivalent to (6.34) - (6.36).

As discussed earlier, the buoyancy of the cloudy air at height z, is approximately[4]

$$B(z) \cong T_c - \bar{T} = \frac{h_c(z) - \bar{h}^*(z)}{c_p}, \tag{6.84}$$

where h^* is the saturation moist static energy. Because more rapidly entraining clouds lose their buoyancy at lower levels, in effect the cloud types differ according to their cloud-top heights, for a given sounding. The cloud top occurs at level p, where

$$B(\hat{p}) \approx 0. \tag{6.85}$$

This equation can be used to find p, after the in-cloud sounding has been determined using (6.71) - (6.76).

To determine the entrainment rate, AS assumed that

$$E = \lambda M_c, \tag{6.86}$$

where λ, which is called the fractional entrainment rate and has the units of inverse length, is assumed to be a constant for each cloud type. Larger values of λ mean stronger entrainment; $\lambda = 0$ means no entrainment; $\lambda < 0$ has no physical meaning and so is not allowed. For a given sounding, clouds with smaller values of λ (weaker mixing) will have higher tops. Because λ is assumed to be a constant, the solution of (6.71) gives an exponential profile for $\eta(\lambda, z)$, from the cloud-base level to the cloud top level.

For simplicity, AS assumed that detrainment occurs only at cloud top.[5] This means that the mass flux jumps discontinuously to zero at cloud top. Below the cloud-top, we have entrainment but no detrainment, so that (6.71) reduces to

---

4. Virtual temperature and ice effects can easily be included in this analysis but have been omitted here for simplicity.

5. Lord (1978) investigated the effects of detrainment distributed continuously along the sides of the cloud, and found that they are negligible.

$$\frac{\partial}{\partial z} M_c(z) = E(z) . \tag{6.87}$$

By combining (6.71) and (6.71), and using the assumption that λ is a constant for each cloud type, we see that

$$M_c(z, \lambda) = M_B(\lambda) \exp(\lambda z) , \tag{6.88}$$

where $M_B(\lambda)$ is the "cloud-base mass flux," which can vary among cloud types but is not a function of height. We define a normalized mass flux, denoted by $\eta(\lambda, z)$; the normalization is in terms of the cloud-base mass flux:

$$M_c(z, \lambda) \equiv M_B(\lambda) \eta(\lambda, z) . \tag{6.89}$$

Note that by virtue of its definition, $\eta(\lambda, z_B) = 1$; here z_B is the cloud-base height.

To determine the intensity of convective activity, AS proposed a "quasi-equilibrium" hypothesis, according to which the convective clouds quickly convert whatever moist convective available potential energy is present in convectively active atmospheric columns into convective kinetic energy. The starting point for the quasi-equilibrium closure is the recognition that cumulus convection occurs as a result of moist convective instability, in which the potential energy of the mean state is converted into the kinetic energy of cumulus convection.

AS defined the "cloud work function," A, for a cumulus subensemble, as a vertical integral of the buoyancy of the cloud air with respect to the large-scale environment:

$$A(\lambda) = \int_{z_B}^{z_D(\lambda)} \frac{g}{c_P \bar{T}(z)} \eta(z, \lambda) [s_{vc}(z, \lambda) - \bar{s}_v(z)] dz . \tag{6.90}$$

Here $z_D(\lambda)$ is the height of the detrainment level for cloud type λ; and s_v denotes the virtual static energy. From (6.90) we see that *the function* $A(\lambda)$ is a property of the large-scale environment. A positive value of $A(\lambda)$ means that a cloud with fractional entrainment rate λ can convert the potential energy of the mean state into convective kinetic energy. For $\lambda = 0$, $A(\lambda)$ is equivalent to the convective available potential energy (CAPE), as conventionally defined.

Numerical models use the conservation equations for thermodynamic energy and moisture to predict $T(z)$ and $q(z)$, from which $A(\lambda)$ can be determined; therefore, these models indirectly predict $A(\lambda)$. By taking the time derivative of (6.90), and using the conservation equations for thermodynamic energy and moisture, AS showed that

$$\frac{d}{dt}A(\lambda) = J(\lambda)M_B(\lambda) + F(\lambda) . \tag{6.91}$$

The JM_B term of (6.91) represents all of the terms involving *convective processes, each of which turns out to be proportional to* M_B. Note, however, that Eq. (6.91) is written in simplified form. The JM_B term actually represents an integral over cloud types, and is written here as a product merely to simplify the discussion. The quantity $J(\lambda)$ symbolically represents the kernel of the integral, which is a property of the large-scale sounding; see AS for details. The JM_B term of (6.91) tends to reduce $A(\lambda)$, because cumulus convection stabilizes the environment, so that $J(\lambda)$ is usually negative. Keep in mind that an equation like (6.91) holds for each cumulus subensemble.

The $F(\lambda)$ term of (6.91) represents what AS called the "large-scale forcing," i.e. the rate at which the cloud work function tends to increase with time due to a variety of processes including:

- horizontal and vertical advection by the mean flow;
- the surface turbulent fluxes of sensible and latent heat, and the rate of change of the planetary boundary-layer depth;
- radiative heating and cooling;
- precipitation and turbulence in stratiform clouds.

Note that some of these "forcing" processes, e.g. those involving boundary-layer turbulence and stratiform clouds, are themselves parameterized processes that may involve fluctuations on small spatial scales; for this reason it seems inappropriate to describe the collection of processes that contribute to F as "large-scale;" a better term would be "non-convective."

AS assumed quasi-equilibrium (QE) of the cloud work function, i.e.

$$\frac{d}{dt}A(\lambda) = JM_B(\lambda) + F(\lambda) \cong 0 \text{ when } F(\lambda) > 0 . \tag{6.92}$$

Eq. (6.92) means that the moist convective instability generated by the forcing, $F(\lambda)$, is very rapidly consumed by cumulus convection, i.e. the two terms on the right-hand side of (6.92) *approximately* balance each other. In a steady-state situation, this balance is of course trivially satisfied, by definition. The physical content of (6.92) is, therefore, the assertion that near-balance is maintained *even when* $F(\lambda)$ *is varying with time*, provided that the variations of $F(\lambda)$ are sufficiently slow. The cumulus ensemble thus closely follows the lead of the forcing, like a defensive basketball player (the convection) playing man-to-man against an offensive player (the forcing). Keep in mind, however, that the forcing depends on the large-scale circulation, which is strongly affected by the convection, just as the play of an offensive basketball player is strongly affected by the moves of his or her defensive opponent. We should not imagine that the forcing is "given" and that the convection just

meekly responds to it. The convection and the forcing evolve together according to the rules defined by the combination of large-scale dynamics and cloud dynamics.

The QE approximation is expected to hold if τ_{LS}, the *time scale for changes* in $F(\lambda)$, is much longer than the "adjustment time," τ_{adj}, required for the convection to consume the available CAPE; this allows the convection to keep up with the changes in $F(\lambda)$. AS introduced the concept of τ_{adj} by describing what would happen if a conditionally unstable initial sounding were modified by cumulus convection, without any forcing to maintain the CAPE over time; they asserted that the CAPE would be consumed by the convection (i.e. converted into convective kinetic energy) on a time-scale that they *defined* as τ_{adj} and estimated to be on the order of a couple of hours. Just such an unforced convective situation has been numerically simulated by Soong and Tao (1980) and others, using high-resolution cloud models; their results are consistent with the scenario of AS. If the adjustment time is on the order of 10^3 to 10^4 s, then use of (6.92) is justified, as an approximation, for the simulation of "weather" whose time scale is on the order of one day or longer, i.e. at least one order of magnitude longer than τ_{adj}.

By using (6.92), together with

$$|JM_B| \sim \frac{A}{\tau_{adj}}, \tag{6.93}$$

AS found that

$$A \sim \tau_{adj} F \ll \tau_{LS} F, \tag{6.94}$$

where τ_{LS} is the time-scale on which the forcing itself is varying. This means that the cloud work function is "small" compared to $\tau_{LS} F$, which is the value that the cloud work function would take if the forcing acted without opposition over a time scale τ_{LS}. Although we should expect to see day-to-day variations of A, we should not expect to see values as large as $\tau_{LS} F$. This means that A is trapped in the range of values between zero (since by definition A cannot be negative) and $\tau_{adj} F$. In this sense, A is "close to zero" (see also Xu and Emanuel, 1989)[6].

[6] Here an earthy analogy, suggested by the pastoral life in Fort Collins, may help. Think of *A* as a a measure of the length of the grass in a field, the convective clouds as a herd of sheep, and the forcing as an irrigation system controlled by a large-scale dynamicist. The sheep eat the grass as quickly as it grows, so that the grass is always short, no matter how generous the supply of water. The sheep are white and fluffy, like convective clouds, and one can even find analogs, in this parable, to the precipitation process.

Based on the analysis above, it can be asserted that the cloud work function (or the CAPE) "is quasi-invariant with time," i.e. that

$$\frac{dA}{dt} \cong 0 , \tag{6.95}$$

which is a short-hand form of Eq. (6.92); and that "the CAPE is small" in convectively active regimes, i.e.

$$A \cong 0 , \tag{6.96}$$

which is a short-hand form of Eq. (6.94). A sounding for which $A \cong 0$ tends to follow a saturated moist adiabat, throughout the depth of the convective layer. This provides a rationalization for Manabe et al.'s assumption that the lapse rate cannot exceed 6.5 K km^{-1}.

Unfortunately, because (6.95) and (6.96) are short-hand forms, they are subject to misinterpretation. For example, data like those shown in Fig. 6.13 are sometimes viewed as

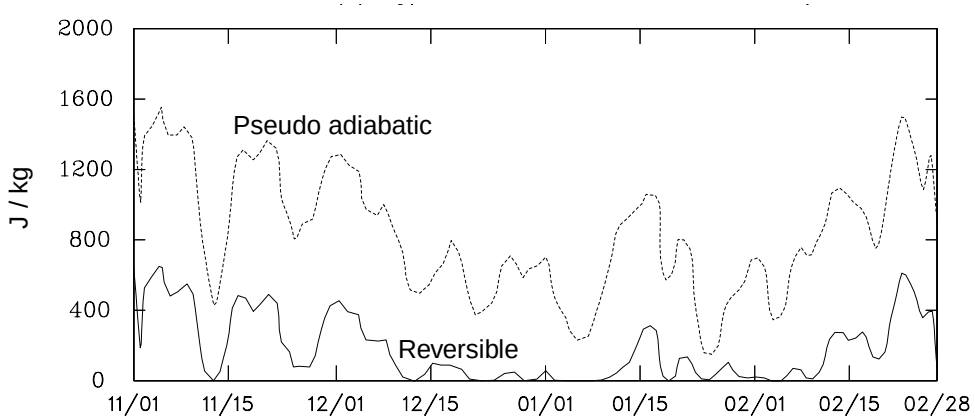

Figure 6.13: Observed time sequence of the CAPE during TOGA COARE, over the Intensive Flux Array. K. Emanuel's code was used to construct these curves. X. Lin of CSU performed the computations.

being inconsistent with QE. It is natural to wonder how the CAPE be described as "quasi-invariant" when it is observed to undergo such "large" changes. This point of view appears to be based on the tacit assumption that when we say that the changes in the CAPE are "small," we mean that they are small compared with the time average of the CAPE. In fact, however, it should be clear from the preceding discussion that this is not what is meant at all. Instead, we mean that the changes in the CAPE are small compared to those that would occur if the convection were somehow suppressed while the non-convective processes continued to increase the CAPE with time. Eq. (6.92) does not imply that A is invariant from day to day, and the observed day-to-day changes in the CAPE, such as those shown in Fig. 6.13, are not necessarily in conflict with QE. What QE does imply is that the changes in the CAPE that we actually see, from day to day, are much smaller than they would be if the negative convective term of (6.92) could somehow be suppressed, so that the positive (under disturbed

conditions) forcing term could have its way with the sounding.

A practical application of (6.92) is to solve it for the convective mass flux as a function of cloud type, λ. After discretization this leads to a system of linear equations (Lord et al. 1982). Although the system is linear, the mass flux distribution function, $M_B(\lambda)$, is required to be non-negative for all λ. This cannot be guaranteed without making additional assumptions (e.g. Hack et al., 1984). An alternative approach that avoids these difficulties was proposed by Randall and Pan (1993) and Pan and Randall (1998).

The QE hypothesis has been observationally tested by Arakawa and Schubert (1974), Lord and Arakawa (1980), Lord (1982), Kao and Ogura (1987), Arakawa and Chen (1987), Grell et al. (1991), Wang and Randall (1994), and Cripe (1994), and Cripe and Randall (2001) among others, using both tropical and midlatitude data. In addition, idealized tests of QE using a high-resolution cloud ensemble model have been performed by Xu and Arakawa (1992).

For further discussions of cumulus parameterization see the collections of essays edited by Emanuel and Raymond (1993) and Smith (1998).

6.5 Summary

The observed vertical structure of the atmosphere is controlled, to a remarkable degree, by diabatic processes. For example, the observed height of the tropopause is approximately that predicted by radiative-convective models, which completely ignore the effects of large-scale dynamics. Obviously this does not mean that dynamics is unimportant, but it does suggest that dynamics is strongly constrained by radiation and convection. At the same time, the heating due to radiation, convection, and boundary-layer turbulence is strongly controlled by the general circulation. It is impossible to understand the circulation without understanding the heating, and vice versa. Further discussion is given in later chapters.

Problems

1. Suppose that moist static energy is simply conserved, i.e.

$$\frac{\partial h}{\partial t} = -\nabla\bullet(\mathbf{V}h) - \frac{\partial}{\partial z}(wh). \tag{6.97}$$

The density has been omitted here and throughout the rest of this problem for simplicity. The corresponding continuity equation is

$$0 = -\nabla\bullet\mathbf{V} - \frac{\partial w}{\partial z}. \tag{6.98}$$

a) By using Reynolds averaging, show that

$$\frac{\partial}{\partial t}\bar{h} = -\nabla\bullet(\bar{\mathbf{V}}\bar{h} + \overline{\mathbf{V}'h'}) - \frac{\partial}{\partial z}(\bar{w}\bar{h} + \overline{w'h'}). \tag{6.99}$$

As discussed in the notes, for large-scale averages this can be approximated by

$$\frac{\partial}{\partial t}\bar{h} \cong -\nabla\bullet(\bar{\mathbf{V}}\bar{h}) - \frac{\partial}{\partial z}(\bar{w}\bar{h} + \overline{w'h'}) . \tag{6.100}$$

b) Show that the moist static energy variance, $\overline{h'^2}$, satisfies

$$\frac{\partial}{\partial t}\overline{h'^2} = -\nabla\bullet\left(\bar{\mathbf{V}}\overline{h'^2} + \overline{\mathbf{V}'h'h'}\right) - \frac{\partial}{\partial z}\left(\bar{w}\overline{h'^2} + \overline{w'h'h'}\right) - 2\overline{\mathbf{V}'h'}\bullet\nabla\bar{h} - 2\overline{w'h'}\frac{\partial}{\partial z}\bar{h} . \tag{6.101}$$

For large-scale averages, the time-rate-of-change term of (6.101) is negligible, as are the terms representing horizontal and vertical advection of $\overline{h'^2}$ by the mean flow, as are the other terms involving horizontal derivatives, so that (6.101) can be drastically simplified to

$$0 \cong -\frac{\partial}{\partial z}(\overline{w'h'h'}) - 2\overline{w'h'}\frac{\partial}{\partial z}\bar{h} . \tag{6.102}$$

c) Now suppose that the vertical velocity fluctuations represented by w' are associated with a single family of cumulus updrafts covering fractional area σ. Show that

$$\overline{w'h'} = \sigma(1-\sigma)(w_u - w_d)(h_u - h_d) , \tag{6.103}$$

$$\overline{w'h'h'} = \sigma(1-\sigma)(1-2\sigma)(w_u - w_d)(h_u - h_d)^2 \tag{6.104}$$

where w_u and w_d are the updraft and downdraft velocities, respectively, and h_u and h_d are the corresponding values of the moist static energy.

d) Define a "convective mass flux" by

$$M \equiv \sigma w_u . \tag{6.105}$$

You may assume

$$\sigma \ll 1 , \tag{6.106}$$

and correspondingly that

$$w_u \gg w_d \text{ and } h_d \cong \bar{h}. \tag{6.107}$$

Using (6.106)-(6.105), show that if the convective mass flux is independent of height, then (6.102) can be approximated by

$$-\frac{\partial}{\partial z}(\overline{w'h'}) = M\frac{\partial}{\partial z}\bar{h}. \tag{6.108}$$

Discuss (6.108) as it relates to the ideas on cumulus parameterization presented in the notes.